



DOI: 10.22144/ctu.jen.2017.008

## AN *Ab initio* STUDY OF *CIS*-[*PTCL*<sub>2</sub>(*IPRAM*)(*HPZ*)] BINDING TO BASE PURINES GUANINE AND ADENINE

Bui Thuy Vy, Pham Vu Nhat

College of Natural Sciences, Can Tho University, Vietnam

### Article info.

Received date: 12/05/2016

Accepted date: 30/03/2017

### Keywords

Anticancer, cisplatin, density functional theory, guanine, hydrogen bonding

### ABSTRACT

*Ab initio* calculations are employed to examine interactions of hydrolysis products of cisplatin and a novel derivative *cis*-[PtCl<sub>2</sub>(iPram)(Hpz)] with the purine base sites of DNA using guanine and adenine as model reactants. Thermodynamic parameters, electronic structures, bonding characteristics and spectroscopic properties of the resulting complexes are investigated in the framework of density functional B3LYP method along with correlation-consistent basis sets. The computed results show that these interactions are dominated by electrostatic effects, namely H-bond contributions, and there exists a flow charge from H atoms of ligands to the base. Another remarkable finding is that the replacement of ammine groups by larger ones accompanies with a somewhat moderate reaction between Pt<sup>II</sup> and the nucleobases.

Cited as: Vy, B. T., Nhat, P. V., 2017. An *Ab initio* study of *cis*-[PTCL<sub>2</sub>(Ipram)(Hpz)] binding to base purines guanine and adenine. Can Tho University Journal of Science. Vol 5: 65-79.

## 1 INTRODUCTION

Cisplatin or *cis*-diamminedichloroplatinum(II) (*cis*-DDP) is a widely-used antitumor drug that has been particularly successful in treating various fatal diseases, including testicular, ovarian, head and neck cancers (Gordon and Hollander, 1993; Weiss and Christian, 1993; Howell, 2013). Unfortunately, the drug does have many limitations, for example, several side effects (such as nausea, ear damage, or vomiting) or both intrinsic and acquired resistance (Von Hoff *et al.*, 1978; Fuertes *et al.*, 2003; Jakupc *et al.*, 2003). Therefore, during recent decades, many efforts have been devoted to the exploitation of alternative platinum complexes in order to limit these drawbacks (Hegmans *et al.*, 2004).

However, finding analogous compounds that outperform cisplatin is an extremely difficult task, not only because of the diversity of the compositions, structures and properties of replaced ligands, but also the lack of quantitative atomic level infor-

mation about the features controlling Pt-DNA interactions. Indeed, thousands of platinum compounds have been synthesized so far (Weiss and Christian, 1993; Wong and Giandomenico, 1999), but only few new agents such as oxaliplatin, carboplatin, and nedaplatin have been registered worldwide and entered clinical practice (Boulikas *et al.*, 2007). In this context, a thorough understanding of interactions between the Pt and DNA building blocks is thought to be helpful in designing cisplatin analogues.

In recent times, quantum chemical calculations have been widely used and made significant contributions to a deeper understanding of the interaction mechanisms between cisplatin and DNA (Kozelka and Chottard, 1990; Kozelka *et al.*, 1993). Using Hartree-Fock (HF) model in conjunction with the minimal basis set STO-3G, Kozelka and co-workers were early able to reproduce some structural patterns of *cis*-DDP–base DNA. Other remarkable results on structural aspects of the

complexes between platinum and biomolecules come from the Carloni group (Carloni *et al.*, 1995; Carloni *et al.*, 2000), based on the application of the density functional theory (DFT). The hydrolysis of cisplatin and some features of the changes in electronic structure including the influence of platinum on base pairs, or the proton affinity have also been intensively studied at different levels of theory (Burda *et al.*, 2001; Zhang *et al.*, 2001; Hill *et al.*, 2002; Monjardet-Bas *et al.*, 2002; Burda *et al.*, 2003). Recently, a combined IRMPD, MS/MS and theoretical study on the interactions of cisplatin and base purines was intensively examined with the aim of providing an accurate characterization of the resulting complexes (Chiavarino *et al.*, 2013).

In this work, we perform a systemic examination on the interactions between a novel derivative of cisplatin, (i.e. *cis*-[PtCl<sub>2</sub>(*i*Pram)(Hpz)], where *i*Pram is isopropylamine and Hpz is pyrazole), and the base purines based on DFT calculations. The interactions of cisplatin with the nucleobase are also revisited for a comparison. Though geometric parameters or spectroscopic information could be sufficiently collected by experimental techniques, it is more difficult to combine structural data with energetic properties using only such traditional observations. Advanced quantum chemical methods become potential and effective tools to connect such fundamental link.

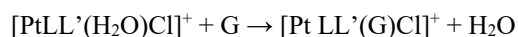
## 2 COMPUTATIONAL METHODS

All calculations are performed using the Gaussian 09 suite of program (Frisch *et al.*, 2009) in the framework of density functional theory (Hohenberg and Kohn, 1964). The hybrid B3LYP functional in conjunction with the correlation consistent cc-pVTZ-PP and cc-pVTZ basis sets is employed for geometry optimization and energetic calculations as well. The basis set with an effective core potential (ECP) cc-pVTZ-PP (Peterson *et al.*, 2003) is applied for platinum, while the all electrons cc-pVTZ basis set is used for the non-metals.

The ECP cc-pVTZ-PP basis set already included relativistic effects that are very crucial in treatment of heavy elements like platinum. Harmonic vibrational frequencies are also calculated to confirm the character of optimized geometries as local minima or transition states on the potential energy surface, and to estimate the zero-point vibrational energy (ZPE) corrections. The natural bond orbital (NBO) charges of atoms are computed using the NBO5.G code (Glendening *et al.*, 2001). We exploit NBO charges for electron population analysis instead of Mulliken charges because the former are expected to be more reliable (Joshi *et al.*, 2006).

It has been confirmed that after entering the cell by passive diffusion through the cell membrane cisplatin undergoes spontaneous hydrolysis *via* nucleophilic substitution of chloride with water to form cationic complexes [Pt(NH<sub>3</sub>)<sub>2</sub>(H<sub>2</sub>O)Cl]<sup>+</sup> and [Pt(NH<sub>3</sub>)<sub>2</sub>(H<sub>2</sub>O)<sub>2</sub>]<sup>2+</sup> (Davies *et al.*, 2000). This process is a fundamental step determining the anticancer activity of cisplatin as it leads to reactive metabolites that ultimately give rise to DNA adducts (Monjardet-Bas *et al.*, 2003). Both complexes can be substituted easily by donor ligands like nitrogen-containing bases of DNA with the loss of water, but it is currently unclear whether the mono-aqua or diaqua species to be more important (Baik *et al.*, 2003).

In this work, we firstly probed the interactions of the mono-aqua cation [Pt(NH<sub>3</sub>)<sub>2</sub>(H<sub>2</sub>O)Cl]<sup>+</sup> with guanine and adenine at various binding sites. Then detailed computations will be performed to examine the interactions of both [Pt(*i*Pram)(Hpz)(H<sub>2</sub>O)Cl]<sup>+</sup> and [Pt(*i*Pram)(Hpz)(H<sub>2</sub>O)<sub>2</sub>]<sup>2+</sup> cations with guanine and adenine, but we just pay attention to the dominating preference for initial anchor. The exchange-ligand energies (E<sup>T</sup>) of these complexes with guanine and adenine are computed based on following processes:



Where L, L' are *i*Pram and Hpz ligands. As for a convention, a negative value of E<sup>T</sup> corresponds to a favorable interchange, but the selectivity is low. In addition, this parameter can be used to evaluate the relative stability of a specific Pt-guanine and Pt-adenine complexes.

## 3 RESULTS AND DISCUSSION

### 3.1 Interactions of [Pt(NH<sub>3</sub>)<sub>2</sub>(H<sub>2</sub>O)Cl]<sup>+</sup> with guanine and adenine

Guanine and adenine are two main nucleobases found in both DNA and RNA. The molecules have several possible binding sites with the transition metal, such as two nitrogen atoms N3 and N7, and the carbonyl oxygen atom (Metcalf and Thomas, 2003). In addition to these traditional anchoring sites, complexes with N1-H tautomers are also considered. The optimized structures of cisplatin – guanine adducts resulting from these binding sites of guanine are presented as PtGN7, PtGN3, PtGN1, and PtGO. Table 1 reports relative energies, hydrogen bond lengths, distances of Pt – guanine for the studied conformers.

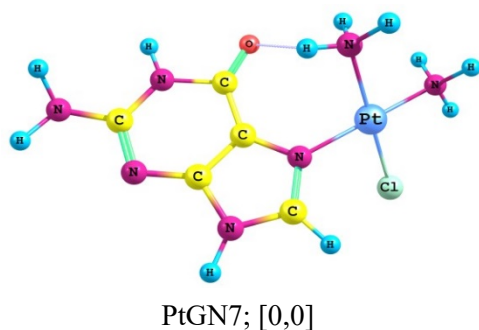


**Fig. 1: The most stable form of  $[\text{Pt}(\text{NH}_3)_2(\text{G})\text{Cl}]^+$  (PtGN7)**

At the B3LYP level, we detect seven configurations for the  $[\text{Pt}(\text{NH}_3)_2(\text{G})\text{Cl}]^+$  complex with G being guanine. As can be seen from Figure 1 and 2, except for N7 position, binding to other sites gives rise to several conformers.

Excluding PtGN3-2, all conformers are stabilized by hydrogen bond between a hydrogen atom of one  $\text{NH}_3$  ligand and the N or O atom of guanine. The PtGN7 is the most stable conformer due to the hydrogen bond length of  $1.757\text{\AA}$ . In contrast, the hydrogen bond is not formed in the least stable PtGN3-1 isomer. This leaves no doubt that hydrogen bond plays a key role on the interactions between cisplatin and guanine. Other remarkable finding is that the N-coordinated sites are more favoured than the O-coordinated position. As expected, the oxo group is a much better hydrogen-bond acceptor than the amino group, thus, the stronger interaction is observed in the Pt – N complexes. In addition, consistent with the hard – soft acid – base prediction, soft acid Pt(II) bonds more strongly with the softer base N than O.

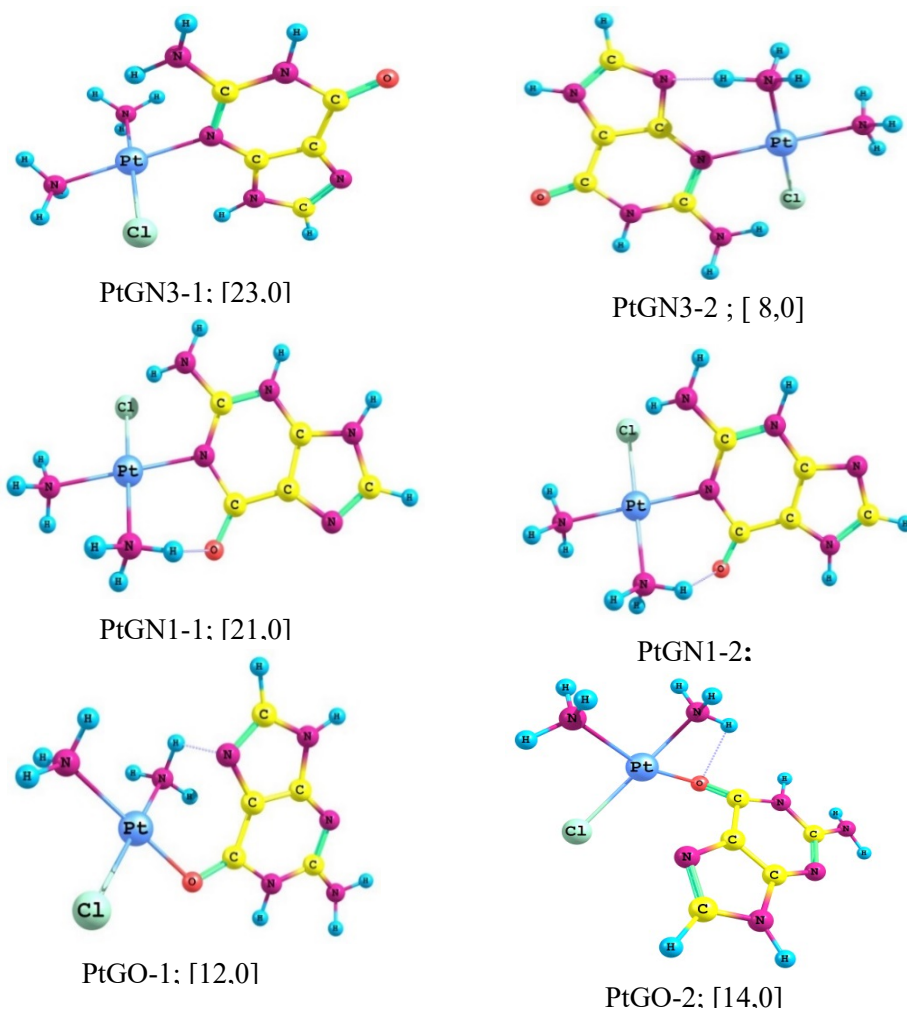


**Fig. 2: The low-lying structures of  $[\text{Pt}(\text{NH}_3)_2(\text{G})\text{Cl}]^+$  complex. The values (kcal/mol) in brackets are relative energies as compared to the lowest energy PtGN7 conformer**

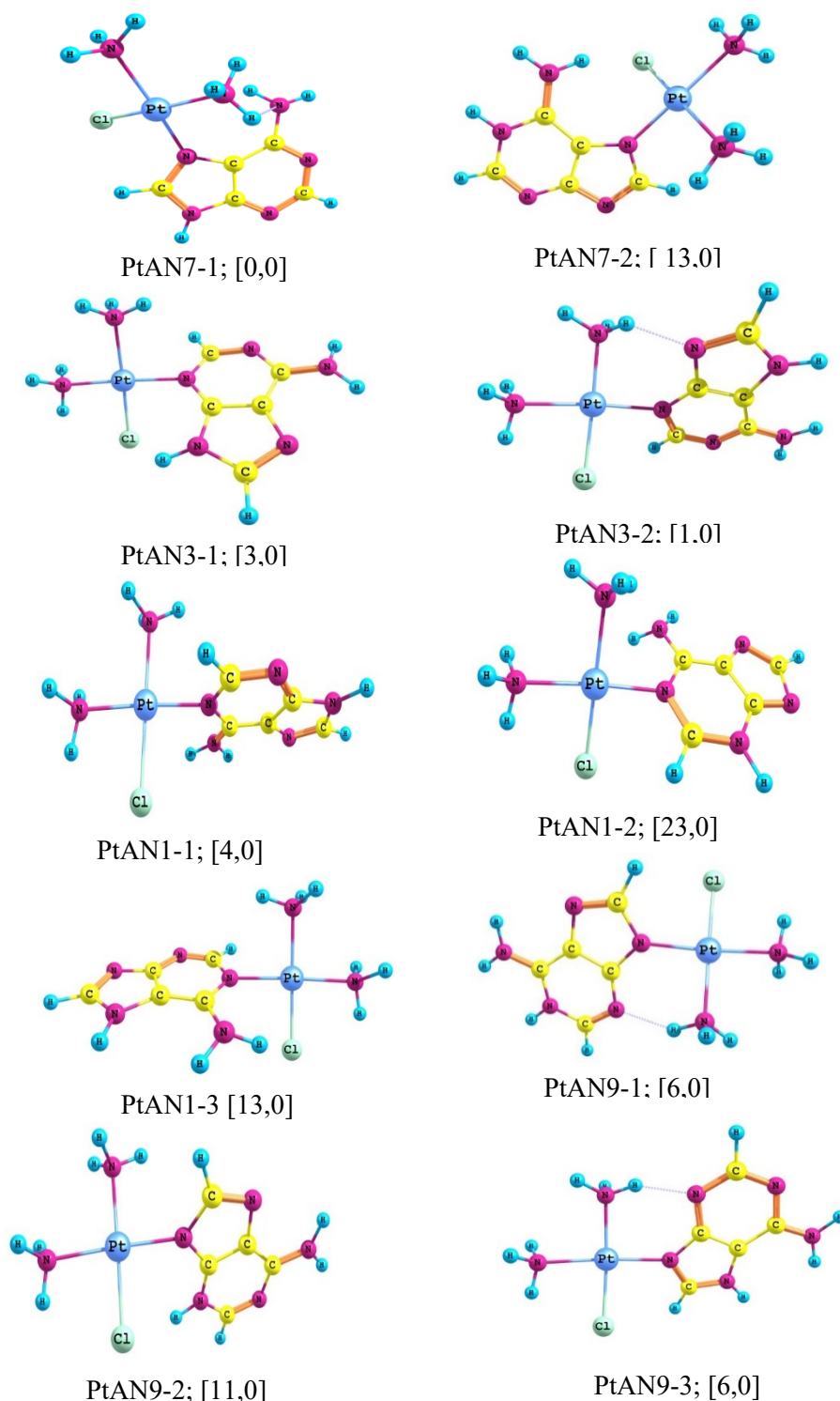


**Fig. 3: Low-lying structures of  $[\text{Pt}(\text{NH}_3)_2(\text{A})\text{Cl}]^+$  complex**

We also identify several configurations for the  $[\text{Pt}(\text{NH}_3)_2(\text{A})\text{Cl}]^+$  complex in which A is adenine. The N1, N3, N7, N9 positions of adenine as displayed in Figure 3 are considered as active sites. The computed results as obtained for Pt – adenine

adducts are reported in Table 2. The PtAN7 is predicted to be the lowest energy structure because there is a hydrogen bond between  $\text{NH}_3$  ligand of cisplatin and N atom of adenine with  $\text{NH} \cdots \text{N}$  distances of 2.015Å.

**Table 1: Relative energies (REs), hydrogen bond lengths, and Pt – guanine ( $r_{Pt-G}$ ) distances of the low-lying structures of  $[Pt(NH_3)_2(G)Cl]^+$  complex**

	RE (kcal/mol)	Hydrogen bond length (Å)	$r_{Pt-G}$ (Å)
PtGN <sub>7</sub>	0.0	1.757	2.049
PtGN3-1	23	-	2.051
PtGN3-2	8	1.975	2.077
PtGN1-1	23	1.892	2.085
PtGN1-2	11	1.859	2.087
PtGO-1	12	1.979	2.060
PtGO-2	14	2.171	2.035

**Table 2: Relative energies (REs), hydrogen bond lengths, and Pt – adenine ( $r_{Pt-A}$ ) distances of the low-lying conformers of  $[Pt(NH_3)_2(A)Cl]^+$  complex**

	RE (kcal/mol)	Hydrogen bond length (Å)	$r_{Pt-A}$ (Å)
PtAN7-1	0	2.015	2.033
PtAN7-2	13	-	2.025
PtAN3-1	3	-	2.041
PtAN3-2	1	1.979	2.055
PtAN1-1	4	-	2.050
PtAN1-2	23	-	2.060
PtAN1-3	13	-	2.052
PtAN9-1	6	2.050	2.033
PtAN9-2	11	-	2.027
PtAN9-3	6	1.860	2.053

Conversely, PtAN1-2 is computed to be the highest-

energy structure. In spite of the hydrogen bonds, PtAN3-2 and PtAN9-1 complexes are less stable than PtAN7-1 because of the low springiness of the hydrogen of NH<sub>3</sub> ligand of cisplatin. The relative energies of the other conformers are given from 3,0 to 23 kcal/mol, where the hydrogen bonds are not presented. Thus, the formation of hydrogen bond is a key factor to stabilize the resulting complexes.

### 3.2 Interactions of $[Pt(iPram)(Hpz)(H_2O)Cl]^+$ with guanine and adenine

The possible isomers detected for cation  $[Pt(iPram)(Hpz)(G)Cl]^+$ , along with their relative energies as computed at the B3LYP level with ZPE corrections, are displayed in Figure 4. The result shows that, excluding the Pt(*iPram*)Hpz(G)-4, all the remaining conformers can form a hydrogen bond *via* the CO group with either NH<sub>2</sub> or NH group.

As shown in Figure 4, the lowest-energy structure of cation  $[Pt(iPram)(Hpz)(G)Cl]^+$  is predicted to be Pt(*iPram*)Hpz(G)-1. This form is stabilized by an electrostatic interaction between N – H group on pyrazole and O atom of guanine. Conversely, the Pt(*iPram*)Hpz(G)-4 conformer becomes significantly less stable due to lack of a H bond as in Pt(*iPram*)Hpz(G)-1 though both structures are quite similar. These conformers are separated around 6.2 kcal/mol. Thus such a gap can be considered as the energy of hydrogen bond in the  $[Pt(iPram)(Hpz)(G)Cl]^+$  complex.

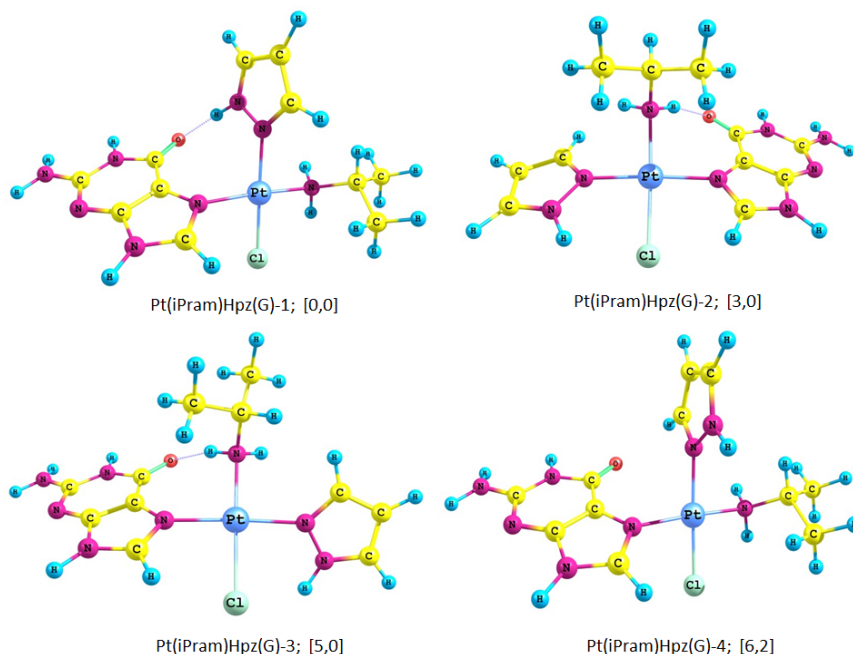


**Fig. 4: The optimized structures of  $[Pt(iPram)(Hpz)(G)Cl]^+$  complex. The values (kcal/mol) in square brackets are their relative energies**

Other conformers, namely Pt(*i*Pram)Hpz(G)-2 and -3 in Figure 4, are estimated to be around 3.0 – 5.0 kcal/mol above the lowest energy state. In these forms, one hydrogen atom of amine group on *i*Pram ligand interacts with the carbonyl oxygen at

the C6 position. This H atom is less flexible than its counterpart on the Hpz ligand. Therefore, the Pt(*i*Pram)Hpz(G)-2 and -3 structures are somewhat higher in energy than the Pt(*i*Pram)Hpz(G)-1.

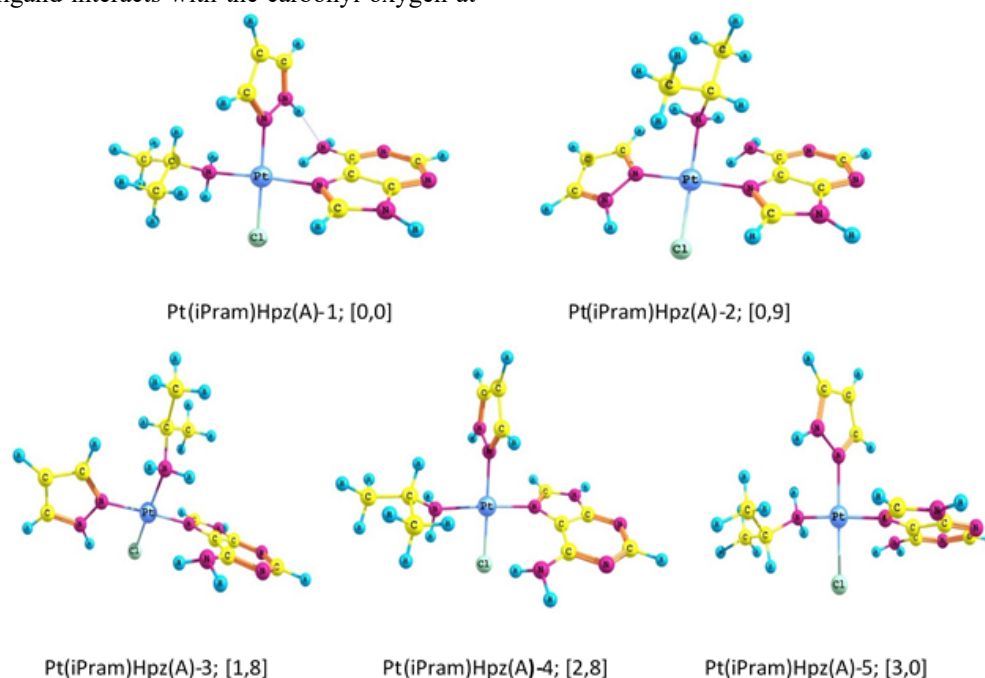


**Fig. 5: The optimized structures of [Pt(*i*Pram)(Hpz)(A)Cl]<sup>+</sup> complex. The values (kcal/mol) in square brackets are their relative energies**

Concerning the interaction of cation [Pt(*i*Pram)(Hpz)(H<sub>2</sub>O)Cl]<sup>+</sup> with adenine, possible structures detected for the adduct are displayed in Figure 5, along with their relative energies computed at the B3LYP/cc-pVTZ-(PP) level with ZPE corrections. The form Pt(*i*Pram)Hpz(A)-1 is computed to the lowest-energy conformation of cation [Pt(*i*Pram)(Hpz)(A)Cl]<sup>+</sup>. This form is again stabilized by a hydrogen bond between N – H group on pyrazole and N atom of adenine. On the contrary, the form Pt(*i*Pram)Hpz(A)-5 is less stable (3.0 kcal/mol) because the H-bond is not created.

**Table 3: Exchange-ligand energy (E<sup>T</sup>) and Pt–N7; NH<sup>\*\*\*</sup>O bond lengths in [Pt(*i*Pram)(Hpz)(G)Cl]<sup>+</sup>**

	ET (kcal/mol)	r <sub>Pt-N7</sub> (Å)	r <sub>NH-O</sub> (Å)
Pt( <i>i</i> Pram)Hpz(G)-1	-37.7	2.06	1.73
Pt( <i>i</i> Pram)Hpz(G)-2	-34.6	2.10	1.81
Pt( <i>i</i> Pram)Hpz(G)-3	-33.9	2.11	1.83
Pt( <i>i</i> Pram)Hpz(G)-4	-32.2	2.06	-

Other conformers, namely Pt(*i*Pram)Hpz(A)-2 and -4 in Figure 5, are estimated to be around 0.9 – 2.8

kcal/mol. Although the Pt(*i*Pram)Hpz(A)-5 structure has highest energy, the energy gap compared to the low-lying isomers is not much substantial. Thus it can be seen that the hydrogen bond becomes not as significant as in [Pt(*i*Pram)(Hpz)(G)Cl]<sup>+</sup>.

Table 3 summarizes computed results obtained for species [Pt(*i*Pram)(Hpz)(G)Cl]<sup>+</sup>. The exchange-ligand energy at the B3LYP/cc-pVTZ/cc-pVTZ-PP level for the mono-aqua complex ranges from -37.7 kcal/mol (Pt(*i*Pram)Hpz(G)-1) to -32.2 kcal/mol (Pt(*i*Pram)Hpz(G)-4). These values can be considered as enthalpy changes of reactions. It follows from Table 3 that if the entropy factor is negligible, these reactions would occur spontaneously and be exothermic. In addition, the absolute values of the reaction energy (above 32 kcal/mol) are high enough for unambiguous conclusions.

At the same level employed, the exchange-ligand energy of *cis*-[Pt(NH<sub>3</sub>)<sub>2</sub>(H<sub>2</sub>O)Cl]<sup>+</sup> with guanine is computed to be around -39.3 kcal/mol. This value is thus more negative than that of the derivative [Pt(*i*Pram)(Hpz)(H<sub>2</sub>O)Cl]<sup>+</sup>. Hence, it can be expected that the former is more willing to exchange the water group by means of a base than the latter.

In other word, the replacement of ammine groups by larger ones such as *i*Pram and Hpz accompanies with a somewhat moderate reaction between Pt<sup>II</sup> and guanine.

In addition, as can be seen from Table 3, there exists a correlation between the exchange-ligand en-

ergy and the distance of H-bond N-H<sup>\*\*\*</sup> O in cation [Pt(*i*Pram)(Hpz)(G)Cl]<sup>+</sup>. The most stable form corresponds to the shortest  $r_{\text{NH}\cdots\text{O}}$  distance and the most negative E<sup>T</sup> value. However, it is not observed any clear correlation between E<sup>T</sup> values and  $r_{\text{Pt-N7}}$  bond lengths.

**Table 4: Exchange-ligand energy (E<sup>T</sup>) and bond lengths Pt-N7; NH<sup>\*\*\*</sup> N in [Pt(*i*Pram)(Hpz)(A)Cl]<sup>+</sup>**

	E <sup>T</sup> (kcal/mol)	Hydrogen bond length (Å)	r <sub>Pt-A</sub> (Å)
Pt( <i>i</i> Pram)Hpz(A)-1	-21.6	2.043	2.043
Pt( <i>i</i> Pram)Hpz(A)-2	-20.7	-	2.034
Pt( <i>i</i> Pram)Hpz(A)-3	-19.8	-	2.034
Pt( <i>i</i> Pram)Hpz(A)-4	-18.8	-	2.044
Pt( <i>i</i> Pram)Hpz(A)-5	-18.6	-	2.042

Table 4 summarizes the computed results for cation [Pt(*i*Pram)(Hpz)(A)Cl]<sup>+</sup>. The exchange-ligand energy at the B3LYP/cc-pVTZ/cc-pVTZ-PP level ranges from -21.6 kcal/mol for Pt(*i*Pram)Hpz(A)-1 to -18.6 kcal/mol for Pt(*i*Pram)Hpz(A)-5. The formation of the NH<sup>\*\*\*</sup> N bond in Pt(*i*Pram)Hpz(A)-1 results in the most stable form and the most negative E<sup>T</sup> value.

### 3.3 Interactions [Pt(*i*Pram)(Hpz)(H<sub>2</sub>O)<sub>2</sub>]<sup>2+</sup> with guanine and adenine

The replacement of one aqua ligand in cation [Pt(*i*Pram)(Hpz)(H<sub>2</sub>O)<sub>2</sub>]<sup>2+</sup> by guanine gives rise to ion [Pt(*i*Pram)(Hpz)(G)(H<sub>2</sub>O)]<sup>2+</sup> with possible structures illustrated in Fig. 6. It can be seen that all the structures are stabilized due to a hydrogen bond, except for the least stable form.

In both Pt(*i*Pram)HpzAq(G)-1 and -2 conformers, a hydrogen bond is established between one hydrogen of the aqua ligand and the oxygen atom at the C6 position. Their relative energy is insignificant, being only around 0.7 kcal/mol. Within the error bar of the computational methods, these conformers can be regarded to be degenerate and each of them can emerge as the ground state.

As expected, the OH group of water is a much better hydrogen-bond donor than the NH group of Hpz. Indeed, the stronger interaction is reflected in the distance of the  $\text{XH}\cdots\text{O}$  bond in platinated gua-

nine adducts as shown in Table 5. The  $\text{OH}\cdots\text{O} = \text{C6}$  hydrogen bond is computed to be 1.45 – 1.49 Å as compared to the value of 1.77 – 1.80 Å for  $\text{NH}\cdots\text{O} = \text{C6}$  in Pt(*i*Pram)HpzAq(G)-3 and 4. These isomers are predicted to be 3.5 – 6.0 kcal/mol higher in energy than the lowest-energy form Pt(*i*Pram)HpzAq(G)-1. When the hydrogen bond is not allowed, the ensuing conformer Pt(*i*Pram)HpzAq(G)-5 becomes least stable, being placed about 9.0 kcal/mol above the ground state. The hydrogen bond is thus expected to contribute approximately 9.0 kcal/mol to the bond energy in the complex [Pt(*i*Pram)(Hpz)(G)(H<sub>2</sub>O)]<sup>2+</sup>.

Several configurations are also detected for the complex [Pt(*i*Pram)(Hpz)(A)(H<sub>2</sub>O)]<sup>2+</sup> as shown in Figure 7. The lowest-energy form Pt(*i*Pram)HpzAq(A)-1 is stabilized by H-bond *via* a hydrogen atom of an aqua ligand with the N atom of adenine, while in the highest-energy isomer Pt(*i*Pram)HpzAq(A)-4, there does not exist any hydrogen bond. At the level of theory employed, the latter is computed to be around 8.0 kcal/mol above the former. The hydrogen bond is thus expected to contribute approximately 8.0 kcal/mol to the bond energy. In addition, as in the complex [Pt(*i*Pram)(Hpz)(G)(H<sub>2</sub>O)]<sup>2+</sup>, interactions between the OH group of water with adenine are stronger than those of NH (Hpz) group.

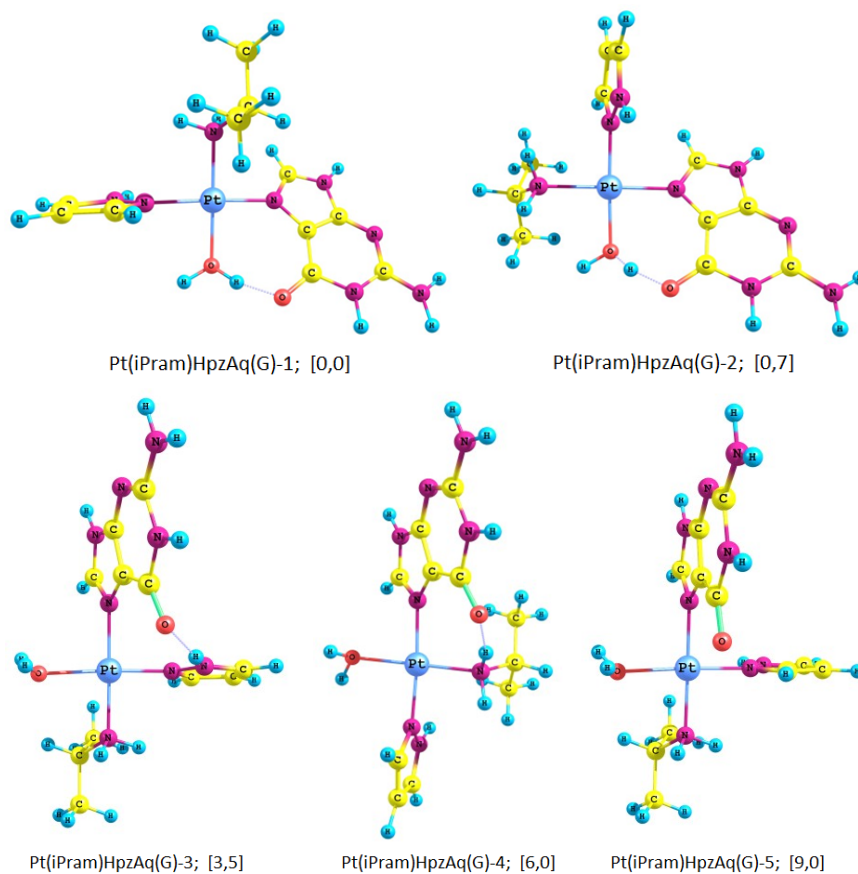


**Fig. 6: Possible structures detected for  $[\text{Pt}(i\text{Pram})(\text{Hpz})(\text{G})(\text{H}_2\text{O})]^{2+}$ . The values (kcal/mol) in square brackets are their relative energies**

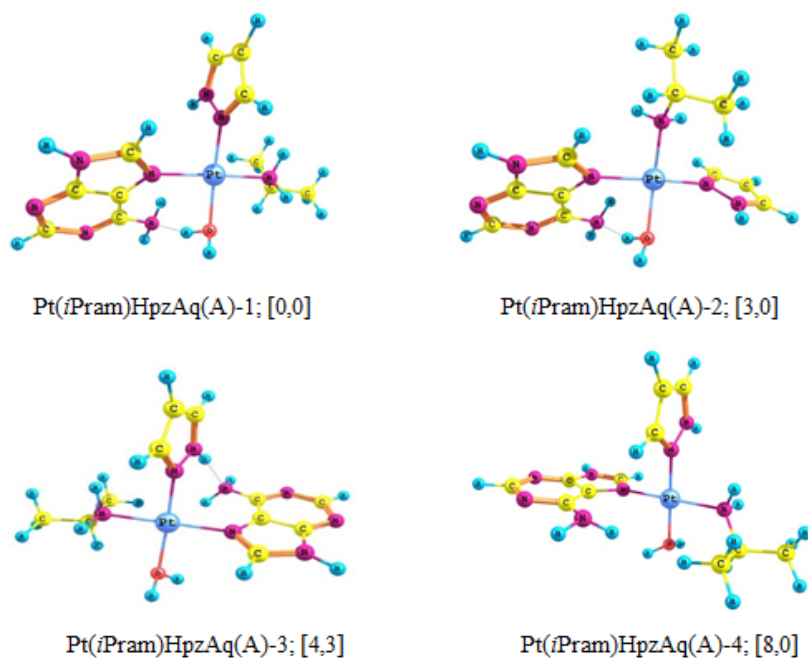


**Fig. 7: The optimized structures of  $[\text{Pt}(i\text{Pram})(\text{Hpz})(\text{A})(\text{H}_2\text{O})]^{2+}$  complex. The values (kcal/mol) in square brackets are their relative energies**

**Table 5: Exchange-ligand energy ( $E^T$ ) and selected geometric parameters in  $[\text{Pt}(i\text{Pram})(\text{Hpz})(\text{G})(\text{H}_2\text{O})]^{2+}$**

	$E^T$ (kcal/mol)	$r_{\text{Pt-N7}}$ (Å)	$r_{\text{XH-O}}$ (Å)
Pt( <i>i</i> Pram)HpzAq(G)-1	-61.1	2.06	1.49
Pt( <i>i</i> Pram)HpzAq(G)-2	-60.5	2.07	1.45
Pt( <i>i</i> Pram)HpzAq(G)-3	-57.7	2.06	1.77
Pt( <i>i</i> Pram)HpzAq(G)-4	-55.3	2.05	1.80
Pt( <i>i</i> Pram)HpzAq(G)-5	-52.3	2.05	-

**Table 6: Exchange-ligand energy ( $E^T$ ) and selected geometric parameters in  $[\text{Pt}(i\text{Pram})(\text{Hpz})(\text{A})(\text{H}_2\text{O})]^{2+}$**

	$E^T$ (kcal/mol)	$r_{\text{XH-N}}$ (Å)	$r_{\text{Pt-N7}}$ (Å)
Pt( <i>i</i> Pram)HpzAq(A)-1	-35.2	1.628	2.065
Pt( <i>i</i> Pram)HpzAq(A)-2	-32.2	1.706	2.055
Pt( <i>i</i> Pram)HpzAq(A)-3	-30.9	1.998	2.056
Pt( <i>i</i> Pram)HpzAq(A)-4	-27.1	-	2.048

The exchange-ligand energies ( $E^T$ ) along with the Pt-N7(G) bond lengths and distances of XH...O (X = O, N) H-bonds are listed in Table 5. The results indicate that if the diaqua complex is used, the platinumation of guanine is more thermodynamically preferable by around 20 kcal/mol. The  $E^T$  values predicted for the diaqua complex vary from -61.1 to -52.3 kcal/mol, as compared to the values of -

**Table 7: The changes in bond lengths ( $\Delta r$ , Å), harmonic frequencies ( $\Delta \nu$ ,  $\text{cm}^{-1}$ ) of X-H bonds when the hydrogen bonds are formed**

Complex	Bonding	$\Delta r$	$\Delta \nu$	Complex	Bonding	$\Delta r$	$\Delta \nu$
Pt( <i>i</i> Pram)Hpz(G)-1	N-H	0.03	-412	Pt( <i>i</i> Pram)HpzAq(G)-1	O-H	0.06	-1220
Pt( <i>i</i> Pram)Hpz(G)-2	HN-H	0.01	-264	Pt( <i>i</i> Pram)HpzAq(G)-2	O-H	0.07	-1352
Pt( <i>i</i> Pram)Hpz(G)-3	HN-H	0.01	-265	Pt( <i>i</i> Pram)HpzAq(G)-3	N-H	0.03	-410
Pt( <i>i</i> Pram)Hpz(G)-4	HN-H	0.00	5.00	Pt( <i>i</i> Pram)HpzAq(G)-4	HN-H	0.02	-383

For instance, the N-H and NH-H distances of Hpz and *i*Pram ligands in  $[\text{Pt}(i\text{Pram})(\text{Hpz})(\text{H}_2\text{O})\text{Cl}]^+$  are computed to be 1,00 and 1,02 Å, respectively, as compared to a value of 1,03 Å in Pt(*i*Pram)Hpz(G)-1 and Pt(*i*Pram)Hpz(G)-2. In agreement with the change in bond lengths, the stretching modes  $\nu(\text{N-H})$  and  $\nu(\text{HN-H})$  are significantly red-shifted to 3238 and 3246  $\text{cm}^{-1}$  when the complexes Pt(*i*Pram)Hpz(G)-1 and -2 are created, while these vibrations are predicted to occur at 3650 and 3510  $\text{cm}^{-1}$  in  $[\text{Pt}(i\text{Pram})(\text{Hpz})(\text{H}_2\text{O})\text{Cl}]^+$ .

Forming the hydrogen bond influences not only X-H bonds but also the carbonyl group of guanine. This phenomenon can be explained by the weakening of the double bond character in the formation of a hydrogen bond, and by the proximity of the

38.3 to -32.2 kcal/mol obtained for the monoqua species (Table 5). Thus, in terms of thermodynamics, cation  $[\text{Pt}(i\text{Pram})(\text{Hpz})(\text{H}_2\text{O})_2]^{2+}$  is more willing to interchange one water ligand with guanine than the monoqua complex  $[\text{Pt}(i\text{Pram})(\text{Hpz})(\text{H}_2\text{O})\text{Cl}]^+$ .

Selected results obtained for the interactions of  $[\text{Pt}(i\text{Pram})(\text{Hpz})(\text{H}_2\text{O})_2]^+$  with adenine are given in Table 6. Again, the complex has larger affinity with adenine than the monoqua counterpart, being from 9 to 14 kcal/mol. The  $E^T$  value of diaqua complexes are predicted from -35,2 to -27.1 kcal/mol, as compared to the values from -21.6 to -18.6 kcal/mol calculated for the monoqua species. Thus, like guanine, adenine also prefers interaction with  $[\text{Pt}(i\text{Pram})(\text{Hpz})(\text{H}_2\text{O})_2]^{2+}$  over  $[\text{Pt}(i\text{Pram})(\text{Hpz})(\text{H}_2\text{O})\text{Cl}]^+$ .

### 3.4 Changes in geometric parameters and vibrational frequencies

As illustrated in Table 7, the introduction of XH...O interaction leads to significant changes in bond lengths and vibrational frequencies of the bonding X-H in systems considered. Our calculations show that as a consequence of a strong electrostatic interaction, bond lengths of N-H and O-H increase by 0.01 - 0.07 Å. Such observations are clearly manifested in the frequency red-shift of the stretching modes  $\nu(\text{N-H})$  and  $\nu(\text{O-H})$ , being around 264 - 1352  $\text{cm}^{-1}$  (Table 7).

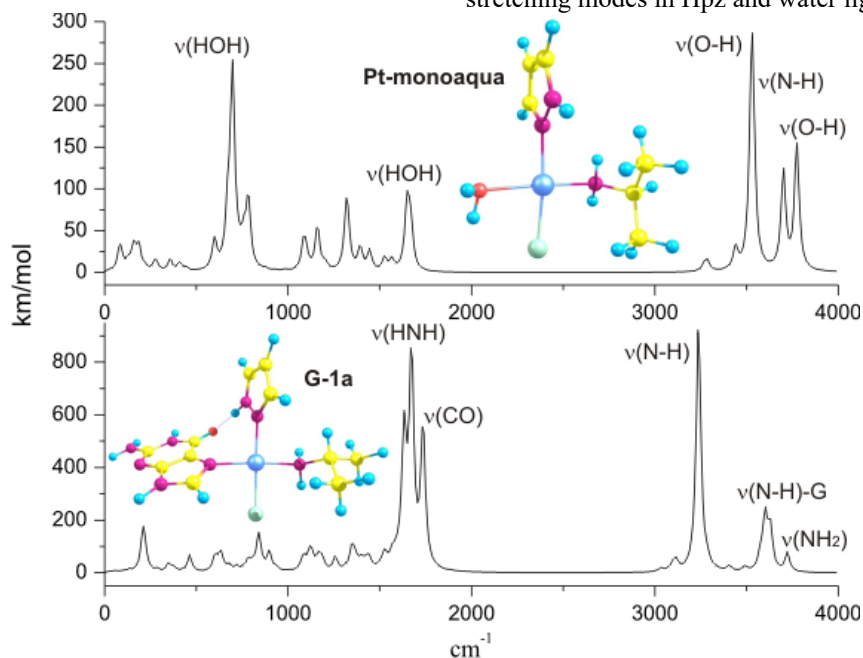
platinum ion. At the B3LYP level, the C=O stretching mode is slightly varied from 1797  $\text{cm}^{-1}$  in free guanine to 1775  $\text{cm}^{-1}$  in Pt(*i*Pram)Hpz(G)-4 (without H-bond). For Pt(*i*Pram)Hpz(G)-1, due to the presence of the hydrogen bond, a much more significant red-shift is observed. Indeed, the  $\nu(\text{C=O})$  mode now shifts to 1736  $\text{cm}^{-1}$ .

Though, the experimental IR spectra for complexes considered in this study have not been published so far, they are reported here as predictions that may allow one to verify the optimal structures when the spectroscopic information is available. Fig. 8 and 9 are plots of the vibrational signatures for lowest energy states of the monoqua, diaqua, and  $[\text{Pt}(i\text{Pram})(\text{Hpz})(\text{G})\text{Cl}]^+$  and  $[\text{Pt}(i\text{Pram})(\text{Hpz})(\text{G})(\text{H}_2\text{O})]^+$  adducts. The results

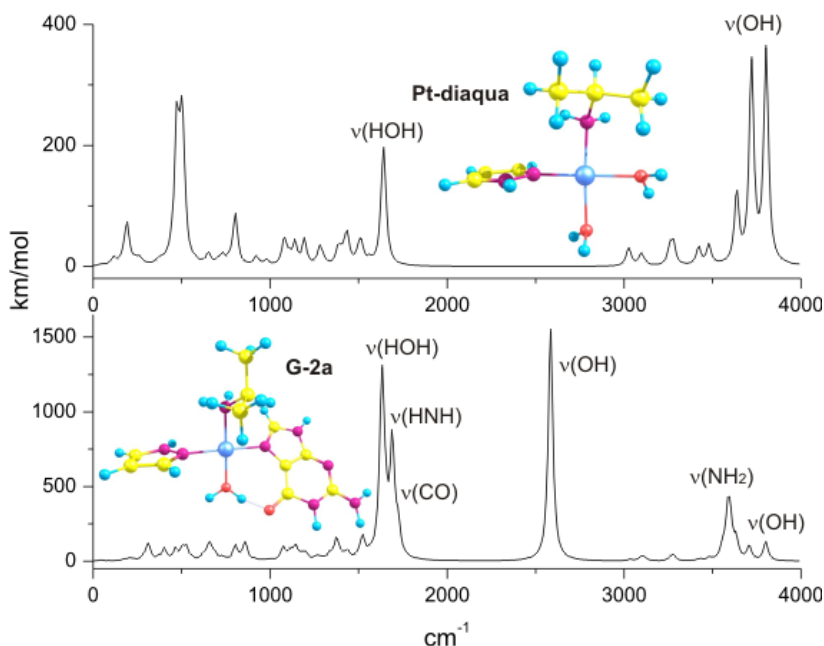
are predicted at the B3LYP/cc-pVTZ/cc-pVTZ-PP level of theory.

Figure 8 and 9 showed that the IR spectra of both the monoqua and diaqua complexes can be classified into two specific regions, namely the fingerprint bands ( $500 - 1700 \text{ cm}^{-1}$ ) and the X-H ( $X = \text{C, N, O}$ ) stretching bands ( $3000 - 3700 \text{ cm}^{-1}$ ). As mentioned above, the vibrational spectra of these

systems are strongly dependent on the nature of surrounded atoms. We actually observe significantly large modifications in band intensities and frequencies of the complexes during the interchange water and guanine ligands. The replacement of a water ligand by a guanine not only modifies the vibrational features in the finger-print region, but also leads to large red-shifts of X-H ( $X = \text{N, O}$ ) stretching modes in Hpz and water ligands.



**Fig. 8: Vibrational signatures of  $[\text{Pt}(i\text{Pram})(\text{Hpz})(\text{H}_2\text{O})\text{Cl}]^+$  (above) and  $[\text{Pt}(i\text{Pram})(\text{Hpz})(\text{G})\text{Cl}]^+$  (below) in their lowest-lying states**



**Fig. 9: Vibrational signatures of  $[\text{Pt}(i\text{Pram})(\text{Hpz})(\text{H}_2\text{O})_2]^{2+}$  (above) and  $[\text{Pt}(i\text{Pram})(\text{Hpz})(\text{G})(\text{H}_2\text{O})]^{2+}$  (below) in their lowest-lying states**

The spectra of both  $[\text{Pt}(i\text{Pram})(\text{Hpz})(\text{H}_2\text{O})\text{Cl}]^+$  and  $[\text{Pt}(i\text{Pram})(\text{Hpz})(\text{H}_2\text{O})_2]^{2+}$  show several intense peaks in the range of  $3000 - 3700 \text{ cm}^{-1}$ . In the computed spectrum of the mono aqua complex, the highest-intensity and highest-frequency bands at  $3631$  and  $3793 \text{ cm}^{-1}$  are the most remarkable features. These bands correspond to the symmetric and asymmetric O – H stretching modes of the water ligand. The other peak at  $3651 \text{ cm}^{-1}$  is associated to the N7–H (Hpz) stretching. For the diaqua complex, two bands at  $3800$  and  $3720 \text{ cm}^{-1}$  are attributed to the symmetric and antisymmetric stretching of OH (water), while the feature around  $3637 \text{ cm}^{-1}$  is assigned to the N7–H (Hpz) stretching. The stretching modes of  $\text{NH}_2$  (*i*Pram) also situate in this region, being predicted to occur at  $\sim 3490 \text{ cm}^{-1}$ , but they are too weak to observe in the computed spectra.

It is clearly seen from Fig. 8 and 9 that the appearance of the hydrogen bond when the  $\text{H}_2\text{O}$  molecule

is replaced by the guanine leads to a significant change in the stretching regions. The predicted spectrum of  $\text{Pt}(i\text{Pram})\text{Hpz}(\text{G})-1$  contains at least four distinct peaks in the range above  $3000 \text{ cm}^{-1}$ . The antisymmetric stretching mode of  $\text{NH}_2$ (guanine) is found to vibrate at  $3723 \text{ cm}^{-1}$ . Other main absorptions estimated at  $3630$ ,  $3575 \text{ cm}^{-1}$  correspond to N9–H and N1–H (guanine) stretches. The highest intensity peak observed at  $3238 \text{ cm}^{-1}$  belongs to the stretching of N–H (Hpz). When the hydrogen bond is not allowed, this vibration is calculated to appear around  $3651 \text{ cm}^{-1}$ . For the isomer  $\text{Pt}(i\text{Pram})\text{HpzAq}(\text{G})-1$ , the hydrogen bond is found between one hydrogen in  $\text{H}_2\text{O}$  and the carbonyl group of guanine. As mentioned above, such interaction in  $\text{Pt}(i\text{Pram})\text{HpzAq}(\text{G})-1$  is much stronger than that in  $\text{Pt}(i\text{Pram})\text{Hpz}(\text{G})-1$ . This is clearly reflected in the IR spectrum of the complex  $\text{Pt}(i\text{Pram})\text{Hpz}(\text{G})-1$ .

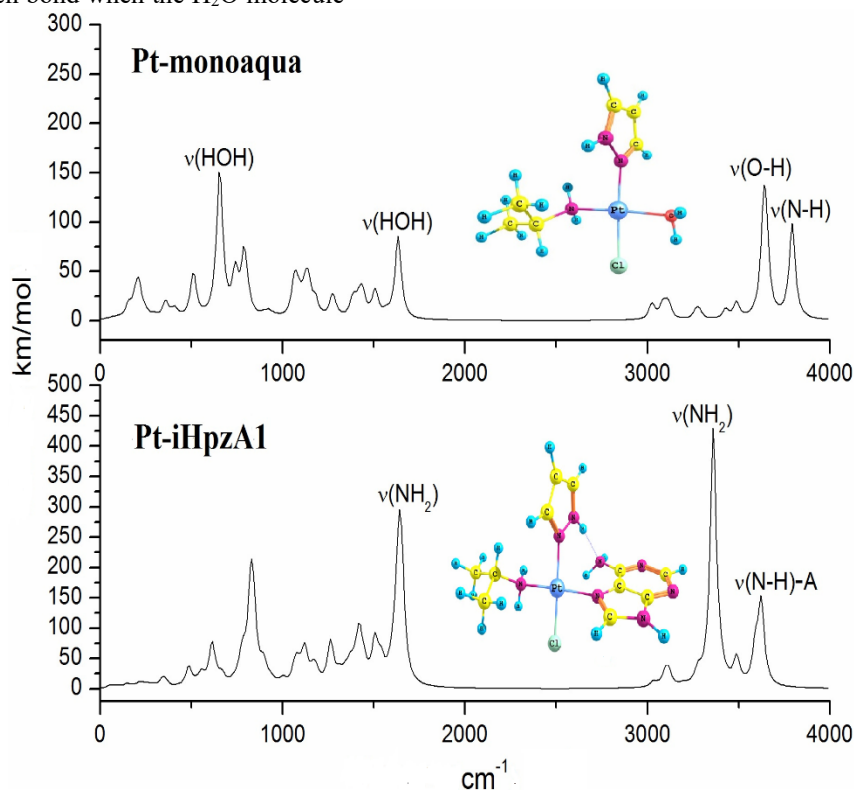


**Fig. 10: Vibrational signatures of  $[\text{Pt}(i\text{Pram})(\text{Hpz})(\text{H}_2\text{O})\text{Cl}]^+$  (above) and  $[\text{Pt}(i\text{Pram})(\text{Hpz})(\text{A})\text{Cl}]^+$  (below) in their lowest-lying states**

In  $\text{Pt}(i\text{Pram})\text{Hpz}(\text{G})-1$ , due to the presence of a hydrogen bond, the O–H symmetric stretching mode of  $\text{H}_2\text{O}$  as found at  $2585 \text{ cm}^{-1}$  is remarkably red-shifted with respect to the unperturbed O–H stretching feature at  $3720 \text{ cm}^{-1}$  in the diaqua complex. In addition to this pronounced band, the symmetric stretches of N9–H and  $\text{NH}_2$  (guanine) of

$\text{Pt}(i\text{Pram})\text{HpzAq}(\text{G})-1$  appears as relatively strong peaks centered at  $3586$  and  $3600 \text{ cm}^{-1}$ . The highest-energy vibration at  $3800 \text{ cm}^{-1}$  is related to the O–H stretching of water ligand that is not involved in hydrogen bonding.

The predicted spectrum of Pt(*i*Pram)Hpz(A)-1 contains at least four distinct peaks in the region above 3000 cm<sup>-1</sup>. The antisymmetric stretching mode of NH<sub>2</sub>(adenine) is observed around 3593 cm<sup>-1</sup>. Other absorptions at 3624 cm<sup>-1</sup> is assigned to N9-H (adenine) stretches. The highest intensity peak at 3361 cm<sup>-1</sup> belongs to the stretching of N-H (Hpz). When the hydrogen bond is not allowed, this vibration is calculated to be around 3648 cm<sup>-1</sup>.

For the isomer Pt(*i*Pram)HpzAq(A)-1, the hydrogen bond is found between one hydrogen in H<sub>2</sub>O and the amine group of adenine (Figure 6). As mentioned above, such interaction in Pt(*i*Pram)HpzAq(A)-1 is much stronger than that in

Pt(*i*Pram)Hpz(A)-1. It is clearly reflected in the IR spectrum of the complex Pt(*i*Pram)Hpz(A)-1.

In Pt(*i*Pram)HpzAq(A)-1, due to the presence of a hydrogen bond, the O-H symmetric stretching mode of H<sub>2</sub>O as found at 2582 cm<sup>-1</sup> is remarkably red-shifted with respect to an unperturbed O-H stretching feature at 3716 cm<sup>-1</sup> in the diaqua complex. In addition to this pronounced band, the relatively strong peaks centered at 3458 and 3591 cm<sup>-1</sup> of Pt(*i*Pram)HpzAq(A)-1 are associated to the symmetric stretches of NH<sub>2</sub> and N9-H (adenine). The highest-energy vibration at 3777 cm<sup>-1</sup> is related to the O-H stretching of water ligand that does not belong to the hydrogen bond.

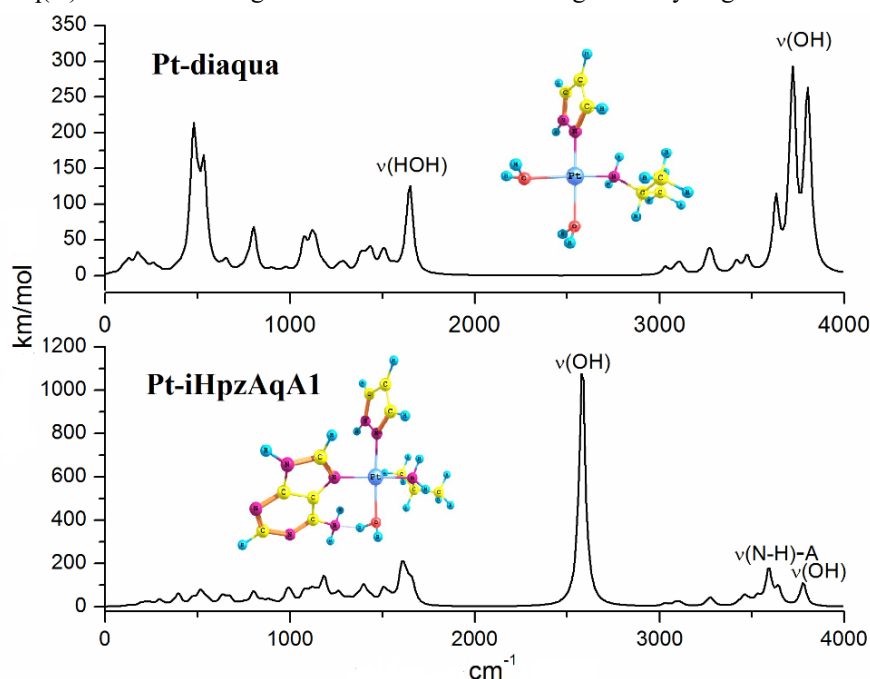


**Fig. 11: Vibrational signatures of [Pt(*i*Pram)(Hpz)(H<sub>2</sub>O)<sub>2</sub>]<sup>2+</sup> (above) and [Pt(*i*Pram)(Hpz)(A)(H<sub>2</sub>O)]<sup>2+</sup> (below) in their lowest-lying states**

### 3.5 Natural bond orbitals analysis

To estimate more precisely the nature of proper hydrogen bonds, we have performed detailed NBO analysis at the same B3LYP/cc-pVTZ/cc-pVTZ-PP level of theory. In the NBO analysis for hydrogen bonding evaluations, the second-order perturbation energy  $E(2)$  is of the particularly interested parameter. It has been pointed out that the larger value of  $E(2)$  for a donor bonding orbital transferred to an acceptor antibonding orbital accompanies with a stronger hydrogen bonding (Reed *et al.* 1988). The  $E(2)$  values for major H-bonds in complexes Pt(*i*Pram)Hpz(G)-1 and Pt(*i*Pram)HpzAq(G)-1 are listed in Table 8.

**Table 8: Second-order perturbation energies  $E(2)$  (donor  $\rightarrow$  acceptor) and NBO charges of atoms involved in hydrogen bonds at the B3LYP/cc-pVTZ/cc-pVTZ-PP level of theory**

Structure	$E(2)$ (kcal/mol)	NBO charge (au)
Pt( <i>i</i> Pram)Hpz(G)-1		
LP(1) O1 $\rightarrow$ $\sigma^*(\text{N8H9})$	6.88	O1 -0.644
LP(2) O1 $\rightarrow$ $\sigma^*(\text{N8H9})$	8.82	H9 +0.454
Pt( <i>i</i> Pram)HpzAq(G)-1		
LP(1) O1 $\rightarrow$ $\sigma^*(\text{O2H9})$	9.43	O1 -0.637
LP(2) O1 $\rightarrow$ $\sigma^*(\text{O2H9})$	38.33	H9 +0.517

Computed results in Table 8 reveal large contributions arising from the interaction of the lone pairs LP(1) and LP(2) of the carbonyl group with  $\sigma^*(N-H)$  and  $\sigma^*(O-H)$  antibonding orbitals. The interactions between the lone pair with the  $\sigma^*(O-H)$  orbital are larger than with the  $\sigma^*(N-H)$ , indicating that Pt(*i*Pram)HpzAq(G)-1 has stronger hydrogen bond than Pt(*i*Pram)Hpz(G)-1.

The second-order perturbation energies in Table 8 in addition shows a presence of interactions derived from the free electron pair LP(1) and LP(2) of the carbonyl group with antibonding orbitals  $\sigma^*(N-H)$  and  $\sigma^*(O-H)$ . Besides, the results indicate that the H-bond of Pt(*i*Pram)HpzAq(G)-1 is much stronger than that of Pt(*i*Pram)Hpz(G)-1. Indeed, the E(2) values in complex Pt(*i*Pram)Hpz(G)-1 are 6.88 and 9.43 as compared to 9.43 and 38.33 kcal/mol of Pt(*i*Pram)HpzAq(G)-1.

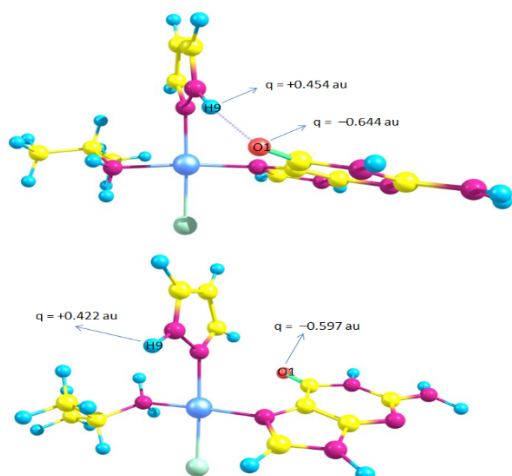


**Fig. 10:** NBO charges of H9 and O1 atoms in Pt(*i*Pram)Hpz(G)-1 (above) and Pt(*i*Pram)Hpz(G)-4 (below)

Since the formation of hydrogen bond is followed by charge distributions, we further examined the NBO charges for the involved atoms to get deeper

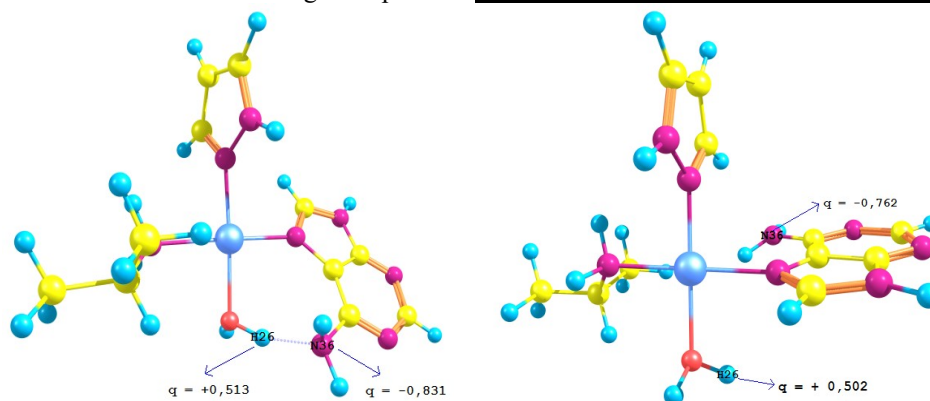


**Fig. 11:** NBO charges of H26 and N36 atoms in Pt(*i*Pram)HpzAq(A)-1 and Pt(*i*Pram)HpzAq(A)-4

insides into the nature of the interaction. The calculated charge distributions for selected complexes Pt(*i*Pram)Hpz(G)-1 and -4 as a result of hydrogen bond are illustrated in Figure 10.

Observed from Figure 10, during the complexation, hydrogen atoms involved in hydrogen bond gain more positive charges, while the oxygen atoms acting as hydrogen acceptor gain more negative charges and the charges on the oxygen atoms acting as hydrogen donor diminish as compared with monomers. Indeed, the charge of H9 in Pt(*i*Pram)Hpz(G)-1 is +0.454 as compared to a value of +0.422 au in Pt(*i*Pram)Hpz(G)-4.

Conversely, the NBO charges of O1 in Pt(*i*Pram)Hpz(G)-1 and Pt(*i*Pram)Hpz(G)-4 are computed to be -0.644 and -0.597 au, respectively, (Figure 10). Thus, there exists an electron flow from H atoms of ligands to atom O6 guanine when hydrogen bonds are formed. Similarly, some selected results on NBO calculations for Pt(*i*Pram)HpzAq(A)-1 and Pt(*i*Pram)HpzAq(A)-4 complexes are summarized in Table 9 and Figure 11.

**Table 9:** Second-order perturbation energies E(2) (donor → acceptor) and NBO charges of atoms involved in hydrogen bonds at the B3LYP/cc-pVTZ/cc-pVTZ-PP level of theory

Structure	E(2) (kcal/mol)	NBO charge (au)
Pt( <i>i</i> Pram)Hpz(A)-1		
LP(1) N34 → $\sigma^*(N24H21)$	9.23	N34 -0.808 H21 +0.442
Pt( <i>i</i> Pram)HpzAq(A)-1		
LP(1) N36 → $\sigma^*(O24H26)$	43.28	N36 -0.831 H26 +0.513

#### 4 CONCLUSIONS

In this study, interactions of hydrolysis products of cisplatin and one of its novel derivative with nucleobase guanine are systematically investigated using quantum chemistry calculations. Density functional B3LYP method combined with correlation consistent basis sets (cc-cc-pVTZ and pVTZ-PP) is employed to examine thermodynamic parameters, electronic structures, bonding characteristics, spectroscopic properties, etc. on a variety of chemical systems, rather than using traditional experimental techniques.

Computed results show that interactions of Pt<sup>II</sup> with guanine prefer to occur at the N7 position. The complex is stabilized due to the formation of strong hydrogen bonds between the H atoms of ammine group and the O6 of guanine. The structures without H-bond is predicted to be around 6.0 – 23 kcal/mol higher in energy. Thus, the interactions between cisplatin and its derivative *cis*-[PtCl<sub>2</sub>(*i*Pram)(Hpz)] with the base purine guanine are dominated by H-bond contributions.

Another significant finding is that the replacement of ammine groups by larger ligands such as *i*Pram, Hpz accompanies with a somewhat moderate reaction between Pt<sup>II</sup> and guanine. The aqua – guanine ligand exchange energies are computed to be –39.3 and –37.7 kcal/mol for *cis*-[Pt(NH<sub>3</sub>)<sub>2</sub>(H<sub>2</sub>O)Cl]<sup>+</sup> and [Pt(*i*Pram)(Hpz)(H<sub>2</sub>O)Cl]<sup>+</sup> respectively. This indicates that the derivatives have a higher selectivity, therefore, they are expected to cause less unexpected effects than cisplatin.

NBO analyses are also conducted to examine more precisely the nature of hydrogen bonds. Our computed results reveal that, during the complexation, the hydrogen atom involved in H-bonds becomes more positive and the oxygen atoms acting as hydrogen acceptor is more negative. Hence, there exists a flow charge from the hydrogen donor to the hydrogen acceptor during forming the H-bond.

The existence of XH...O interaction, in addition, leads to large modifications in bond lengths and vibrational frequencies of the X–H bonds (X = O, N). As a result of strong electrostatic effects, the N–H and O–H bond lengths are increased by 0.01 – 0.07 Å, corresponding to significant frequency red-shifts of the stretching modes  $\nu$ (N–H) and  $\nu$ (O–H), being around 264 – 1352 cm<sup>-1</sup>. Interactions of *cis*-[PtCl<sub>2</sub>(*i*Pram)(Hpz)] with adenine also bring about the same trends in the change of bond lengths and vibrational frequencies of the X–H bonds, i.e. N–H and O–H bonds increase by 0.01 –

0.06 Å and the corresponding frequency red-shifts from 194cm<sup>-1</sup> to 1134 cm<sup>-1</sup>.

Even though the experimental IR spectra for systems considered in this study have not been published so far, they are reported here as predictions that may allow one to verify the optimal structures when the spectroscopic information is available.

#### ACKNOWLEDGEMENT

The authors are grateful to the Interdisciplinary Center for Nanotoxicity, Jackson State University, USA for using computing resources, and to Can Tho University for financial supports.

#### REFERENCES

- Baik, M.H., Friesner R.A., Lippard S.J., 2003. Theoretical study of cisplatin binding to purine bases: why does cisplatin prefer guanine over adenine? *Journal of the American Chemical Society*. 125: 14082-14092.
- Boulikas, T., Pantos, A., Bellis, E., Christofis, P., 2007. Designing platinum compounds in cancer: structures and mechanisms. *Cancer Ther.* 5: 537-583.
- Burda, J.V., Šponer, J., Hrabáková, J., Zeizinger, M., Leszczynski, J., 2003. The influence of N7 guanine modifications on the strength of Watson-Crick base pairing and guanine N1 acidity: comparison of gas-phase and condensed-phase trends. *The Journal of Physical Chemistry B*. 107: 5349-5356.
- Burda, J.V., Šponer, J., Leszczynski, J., 2001. The influence of square planar platinum complexes on DNA base pairing. An ab initio DFT study. *Physical Chemistry Chemical Physics*. 3: 4404-4411.
- Carloni, P., Andreoni W., Hutter, J., Curioni, A., Giannozzi, P., Parrinello, M., 1995. Structure and bonding in cisplatin and other Pt (II) complexes. *Chemical physics letters* 234: 50-56.
- Carloni, P., Sprik, M., Andreoni, W., 2000. Key steps of the cis-Platin-DNA interaction: density functional theory-based molecular dynamics simulations. *The Journal of Physical Chemistry B*. 104: 823-835.
- Chiavarino, B., Crestoni M.E., Fornarini, S., Scuderi, D., Salpin, J.Y., 2013. Interaction of cisplatin with adenine and guanine: A combined IRMPD, MS/MS, and theoretical study. *Journal of the American Chemical Society*. 135: 1445-1455.
- Davies, M.S., Berners-Price, S.J., Hambley, T.W., 2000. Slowing of cisplatin aquation in the presence of DNA but not in the presence of phosphate: improved understanding of sequence selectivity and the roles of mono-aquated and diaquated species in the binding of cisplatin to DNA. *Inorganic chemistry*. 39: 5603-5613.
- Frisch, M., Trucks, G., Schlegel, H.B., Scuseria, G., Robb, M., Cheeseman, J., Scalmani, G., Barone V., Mennucci, B., Petersson, G.E., 2009. Gaussian 09: Gaussian, Inc. Wallingford, CT.
- Fuertes, M.A., Alonso, C., and Pérez, J.M., 2003. Biochemical modulation of cisplatin mechanisms of

- action: enhancement of antitumor activity and circumvention of drug resistance. *Chemical Reviews*. 103: 645-662.
- Glendening, E., Badenhoop, J., Reed, A., Carpenter, J., Bohmann, J., Morales, C., Weinhold, F., 2001. Theoretical chemistry institute. *University of Wisconsin, Madison*.
- Gordon, M., Hollander, S., 1993. Review of platinum anticancer compounds. *Journal of medicine*. 24: 209.
- Hegmans, A., Berners-Price, S.J., Davies, M.S., Thomas, D.S., Humphreys, A.S., Farrell, N., 2004. Long range 1, 4 and 1, 6-interstrand cross-links formed by a trinuclear platinum complex. Minor groove preassociation affects kinetics and mechanism of cross-link formation as well as adduct structure. *Journal of the American Chemical Society*. 126: 2166-2180.
- Hill, G.A., Forde, G., Gorb, L., Leszczynski, J., 2002. cis-Diamminedichloropalladium and its interaction with guanine and guanine-cytosine base pair. *International journal of quantum chemistry*. 90: 1121-1128.
- Hohenberg, P., Kohn, W., 1964. Inhomogeneous electron gas. *Physical review*. 136: B864.
- Howell, S. B., 2013. *Platinum and other metal coordination compounds in cancer chemotherapy*: Springer Science & Business Media.
- Jakupec, M., Galanski, M., Keppler, B., 2003. Tumour-inhibiting platinum complexes—state of the art and future perspectives. In *Reviews of physiology, biochemistry and pharmacology*: Springer, 1-53.
- Joshi, A.M., Tucker, M.H., Delgass, W.N., Thomson, K.T., 2006. CO adsorption on pure and binary-alloy gold clusters: a quantum chemical study. *The Journal of chemical physics*. 125: 194707-194707.
- Kozelka, J.I., Chottard, J.C., 1990. How does cisplatin alter DNA structure?: A molecular mechanics study on double-stranded oligonucleotides. *Biophysical chemistry*. 35: 165-178.
- Kozelka, J.I., Savinelli, R., Berthier, G., Flament, J.P., Lavery, R., 1993. Force field for platinum binding to adenine. *Journal of computational chemistry*. 14: 45-53.
- Metcalfe, C., Thomas, J.A., 2003. Kinetically inert transition metal complexes that reversibly bind to DNA. *Chemical Society Reviews*. 32: 215-224.
- Monjardet-Bas, V., Bombard, S., Chottard, J.C., Kozelka, J., 2003. GA and AG sequences of DNA react with cisplatin at comparable rates. *Chemistry—A European Journal*. 9: 4739-4745.
- Monjardet-Bas, V., Elizondo-Riojas, M.A., Chottard, J.C., Kozelka, J., 2002. A Combined Effect of Molecular Electrostatic Potential and N7 Accessibility Explains Sequence-Dependent Binding of cis-[Pt(NH<sub>3</sub>)<sub>2</sub>(H<sub>2</sub>O)<sub>2</sub>]<sup>2+</sup> to DNA Duplexes. *Angewandte Chemie International Edition*. 41: 2998-3001.
- Peterson, K.A., Figgen, D., Goll, E., Stoll, H., Dolg, M., 2003. Systematically convergent basis sets with relativistic pseudopotentials. II. Small-core pseudopotentials and correlation consistent basis sets for the post-d group 16–18 elements. *The Journal of chemical physics*. 119: 11113-11123.
- Reed, A.E., Curtiss, L.A., Weinhold, F., 1988. Intermolecular interactions from a natural bond orbital, donor-acceptor viewpoint. *Chemical Reviews*. 88: 899-926.
- Von Hoff, D., Schilsky, R., Reichert, C., Reddick, R., Rozenzweig, M., Young, R., Muggia, F., 1978. Toxic effects of cis-dichlorodiammineplatinum (II) in man. *Cancer treatment reports*. 63: 1527-1531.
- Weiss, R.B., Christian, M.C., 1993. New cisplatin analogues in development. *Drugs*. 46: 360-377.
- Wong, E., Giandomenico, C. M., 1999. Current status of platinum-based antitumor drugs. *Chemical reviews*. 99: 2451-2466.
- Zhang, Y., Guo, Z., You, X.-Z., 2001. Hydrolysis theory for cisplatin and its analogues based on density functional studies. *Journal of the American Chemical Society*. 123: 9378-9387.